Spring 5-22-2020

Design of Versatile Feedback Control System Components for Selective Laser Sintering

Thomas Chessman
thomas.chessman@uconn.edu

Design of Versatile Feedback Control System Components for Selective Laser Sintering

by Thomas Chessman
University of Connecticut

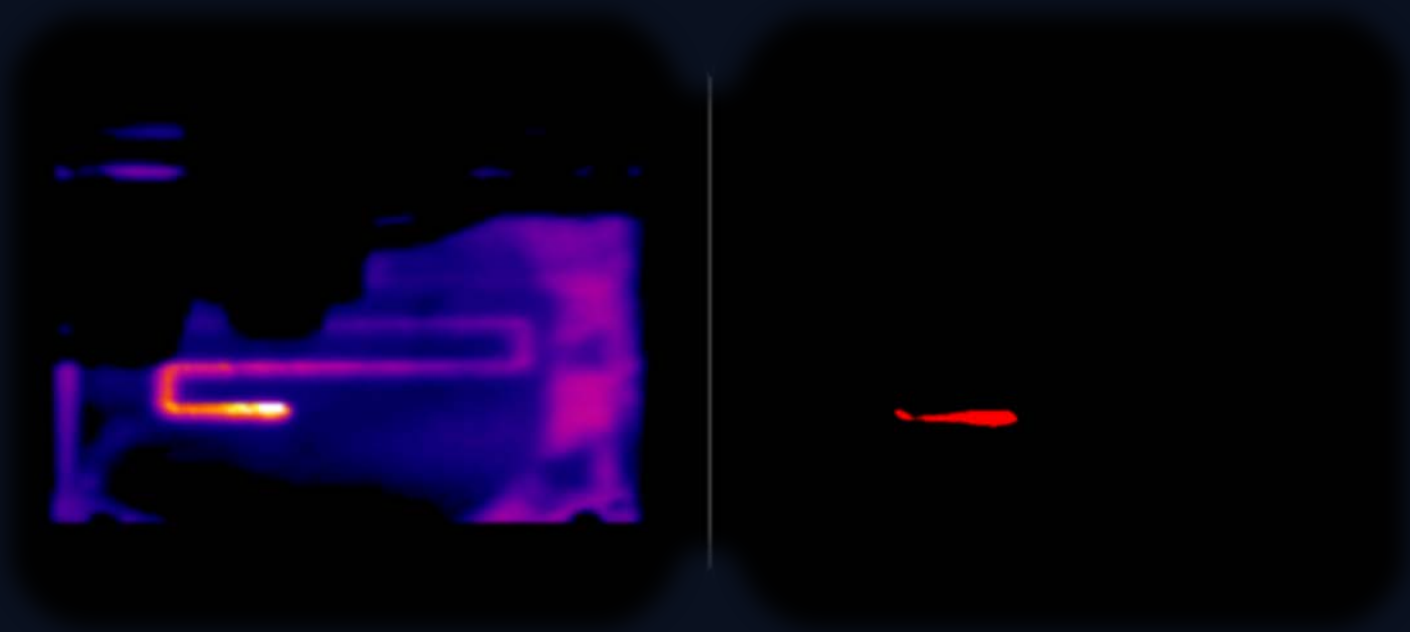

University Scholar Committee:
Professor Chih-Jen Sung, Chair
Professor Song Han
Professor Tai-Hsi Fan

Honors Faculty Adviser:
Professor Horea T. Ilies

Acknowledgements

This project was made possible by the Mechatronics, Automation, and Control Systems Laboratory (MACS Lab) formerly located at University of Connecticut, now at University of Washington. MACS Lab leader, Professor Xu Chen, provided inspiration, resources, and constant support for this project. I am grateful for all the feedback and direction he gave me as the former project committee chair. Other members of the lab, including PhD candidate Dan Wang and PhD candidate Hui Xiao, consistently provided advice, assistance, and a beneficial work environment. Working in MACS Lab was a cornerstone experience of my academic life at University of Connecticut.

I would also like to state my appreciation for all members of the project committee and my honors adviser. Their patience and guidance helped me eventually close this project.

Outside of school, I would specifically like to thank the Hardiman family who donated a blender to the project which was to be used for pulverizing polycaprolactone pellets into powder for sintering.

Finally, special thanks are due to PhD candidate Tianyu Jiang, who relentlessly offered me help throughout the course of this project. I am grateful that he eagerly oversaw my work and gave me the opportunity to assist him in his research.

Abstract

Selective laser sintering (SLS) is an additive manufacturing technique that involves using a laser to fuse powdered material together, layer by layer, in order to create a 3-D product. Despite its numerous benefits over traditional methods of manufacturing, including higher efficiency, versatility, and the ability to process many materials, selective laser sintering suffers from its propensity to generate structural errors during operation.

Feedback control has been shown to improve fabrication quality in other laser-based additive manufacturing techniques when implemented properly. Widespread exploration of applying feedback control in SLS might lead to significant performance improvements in this form of manufacturing.

This project covers the design of versatile feedback control system components for laser-based additive manufacturing machines to aid in the investigation of feedback control in SLS. Two separate SLS testbeds are used as platforms for development to verify that the components can be adapted for use across different machines. Adjustment capabilities are present to allow the investigation of different feedback control strategies and their impact on SLS manufacturing.

Among the components is a sensor consisting of a thermal camera and image analysis program. This sensor component gathers images during the manufacturing process. Properties, such as the size of target temperature regions, can be determined.

Measured values from the sensor are then sent to a controller component. The controller component can make use of any of these measurements as inputs for testing a wide range of different control strategies.

Two different plans for an actuator component are explored specific to the design of each SLS testbed. Both component plans are intended to impact fabrication quality by influencing laser energy density through adjusting a single laser parameter. On one machine, a component strategy is devised that enables laser scan speed adjustments during manufacturing. On the other machine, a modification is formulated that would allow continuous laser power adjustments during system operation. Both actuation plans work by taking advantage of the way each machine processes g-code. The presented actuation strategies require minimal machine hardware additions to implement.

Contents

Equations and Variables

Variable	Description
A_R	Real-world area of temperature region
P_R	Number of pixels in region part of image
P_T	Number of pixels in powder bed image
A_T	Real-world area of powder bed
$u(t)$	Control signal
$e(t)$	Error
t	Time

Variable	Description
K_p	Proportional gain
K_i	Integral gain
K_d	Derivative gain
E_L	Laser energy density
P_L	Laser power
A_L	Laser spot size
S_L	Laser scan speed

List of Figures

1. Introduction

Additive manufacturing is a promising production technique that can provide better fabrication versatility, time efficiency, and resourcefulness compared to traditional methods of manufacturing. The technology can apply material precisely, offering the versatility to produce geometries that would otherwise be impossible using previous fabrication methods. Additive manufacturing can save time by enabling the production of different complex parts from a single machine. Additionally, this method saves resources because it adds material incrementally to form a product rather than cutting excess pieces away as waste.

Despite additive manufacturing's positive attributes, the technology suffers from its inability to reduce error during operation.[1] Production errors manifest themselves in the final product's structure. These errors have largely prevented additive manufacturing's adoption since it is viewed as unreliable and therefore unfit for the creation of end-use products.

Among the most prevalent forms of additive manufacturing that experience unwanted error is Selective Laser Sintering (SLS). This technique involves a laser that thermally fuses powdered material, layer by layer, until a final product is produced. SLS is unique and highly desirable because it offers the ability to manufacture with many different materials including plastics and metals. There are many factors that can influence final part quality in SLS such as properties of the temperature region under the laser where sintering occurs. For example, problems in quality can occur if the temperature beneath the laser gets too hot and the material overheats. [2]

Implementing control systems in laser-based additive manufacturing methods has been shown to deliver improvements in printed geometric quality. The Research Center for Advanced Manufacturing at Southern Methodist University achieved improvements in geometric fabrication accuracy by using a closed loop control system.[3] Researchers at the Catholic University of Leuven also achieved fabrication quality improvements by implementing feedback control in laser-based additive manufacturing. [4] These successes suggest that there is potential for improving laser based additive manufacturing with feedback control systems. More testing in this area is desirable.

This project covers the design of a feedback control system for two separate SLS machines. Focus is placed on the structure of each component in the control system. The intention is that these components might serve as collection of ideas, programs, and strategies to consider when implementing feedback control systems on different laser-based additive manufacturing machines. These components are designed with versatility in mind and meant to allow modification. It is thought that with broad modification possibilities, one might have the capability to extensively explore the potential benefits of feedback control in SLS.

2. SLS Machine Testbeds

Two separate SLS machines, called MACS Machine and Plan-B, are directly targeted with this feedback control project. These machines are designed to serve as testbeds for additive manufacturing research. The software and hardware on both machines can be modified. This makes implementing experimental system additions, like feedback control, straightforward and unconstrained by intentionally inaccessible designs seen onboard some commercial machines.

Both machines take advantage of some of the same feedback control system components developed. Working to implement the project on the two different machines with some of the same components forces these parts of the feedback control system to be more versatile.

Figure 1 shows the two testbed machines. Figure 2 lists the hardware on the machines relevant to this report. Both machines resided in the Mechatronics, Automation, and Control Systems (MACS) Lab at UConn until the lab moved to University of Washington in Fall 2019.

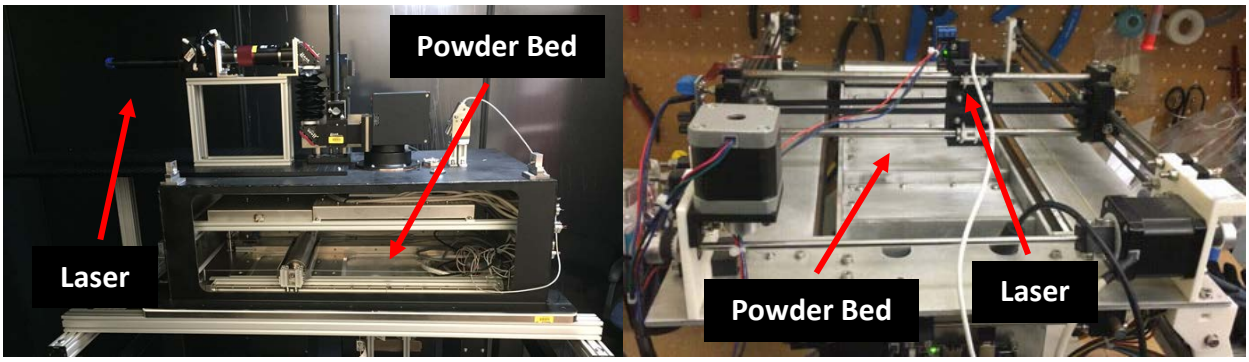

Figure 1: (Left) The MACS Machine is the larger of the two testbeds featuring an 100W CO^2 laser guided onto the powder bed by a galvanometer scanner system. Most of the programming is LabVIEW based. (Right) Plan-B features a 2.2W laser, guided by two motors, positioned over the machine's powder bed. The systems programming is Arduino based. (both pictures) These machines were developed in parallel to this project by PhD student Tianyu Jiang until their disassembly in Fall 2019 when the MACS lab moved.

SLS Testbed	Software / Programming	Hardware
MACS Machine	• LabVIEW • SCANLAB RTC®5 Commands	• Coherent 100W CO2 Laser • SCANLAB RTC®5 Interface Board
Plan-B	• Arduino (C/C++) • I2C Protocol	• J Tech Photonics 2.2W Laser • RepRap Megatronics Board • Devantech USB to I2C Module

Figure 2: Listed are the software and hardware items/environments critical to each machine that are relevant to this report.

3. Feedback Control System Components Overview

The intended position of each component in the feedback control system is outlined in Figure 3. Each item is designed as a separate modular entity. These are linked together to make up the entire control system impacting the SLS manufacturing process.

Sintering characteristics in the SLS Process are observed by a sensor component made up of a thermal camera and image processing program. Thermal images of the sintering region are sent to the image processing program. Temperature region measurement reports from the program are then sent to a control component. Here, the measured sintering characteristics are compared against references. The control mechanism outputs a manipulated variable that is sent to a laser actuation assembly onboard the SLS machine. Laser behavior adjustments are made. The impact of the laser on the sintering process is observed and manufacturing information is fed back into the control system.

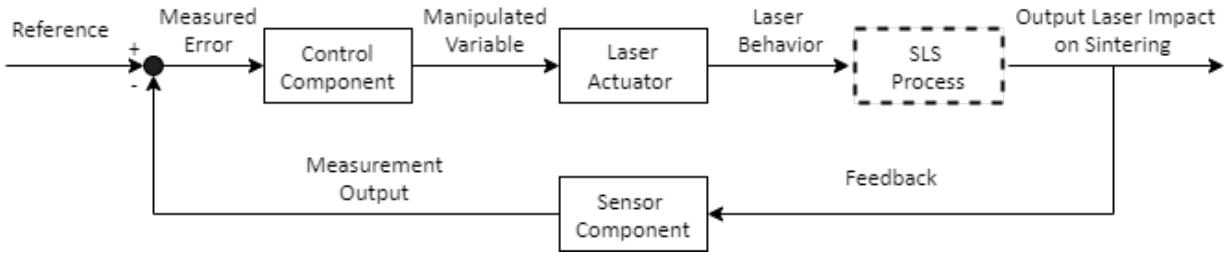

Figure 3: Pictured is the layout of the linked feedback control system. The solid line boxes are control system components impacting the SLS manufacturing process (dotted line box).

4. Software and Materials

Figure 4 shows the materials used or modified to create each component of the feedback control system. LabVIEW is used extensively because of its large selection of virtual instruments geared towards system engineering, ease of integration with hardware (like the thermal camera), and modularity.

Component	Software / Programming	Hardware
Sensor	LabVIEW (Vision Development Module)	FLIR A325 Thermal Camera
Controller	LabVIEW	Nothing modified/added
Plan-B Actuator	MATLAB, Arduino IDE (C/C++)	Nothing modified/added
MACS Machine Actuator	MATLAB, LabVIEW, RTC®5 Commands	Devantech USB to I2C Interface

Figure 4: This chart shows the software environments/packages and hardware used in the development of each component. Hardware on the SLS testbeds that was not physically modified (like the lasers) is not included.

5. Sensor Component Design

In order to measure characteristics of the area heated by laser contact, a sensor component composed of a thermal camera and image processing program is put together. The thermal camera used is a FLIR A325, while the program is built in LabVIEW.

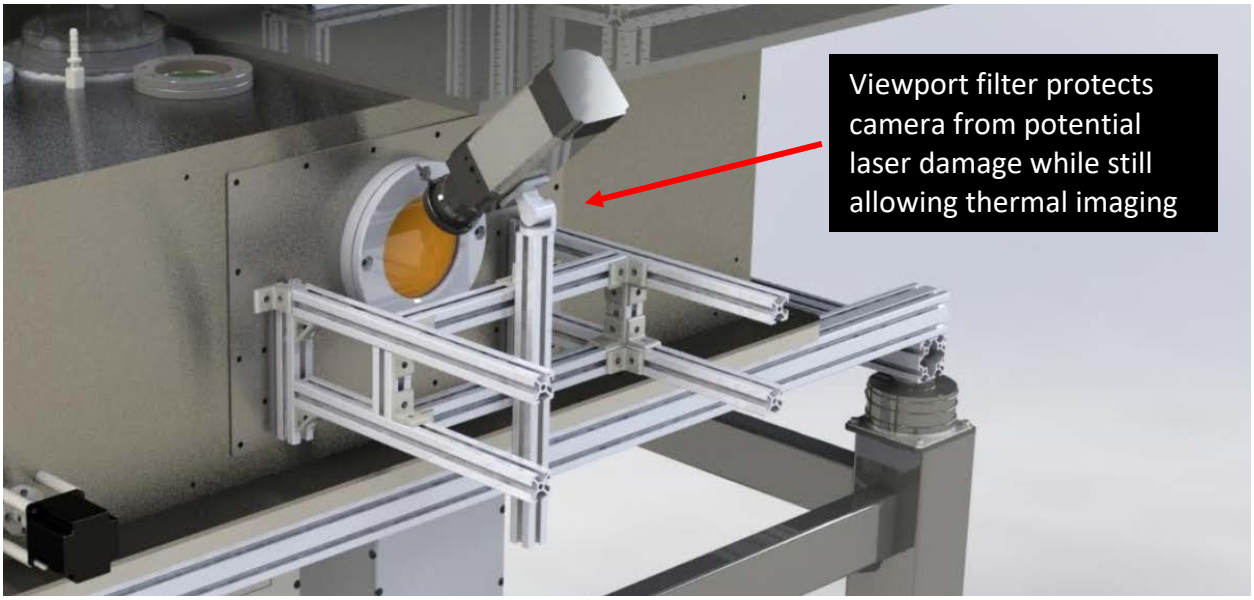

Figure 5: Pictured is the thermal camera's position for viewing the powder bed on the MACS Machine. The camera's displaced angle from a downward view does not stray more than 45^{o}. Excessively angled views degrade the camera's temperature measurement accuracy and require an increased amount of perspective correction.

For both the MACS Machine and Plan-B, the thermal camera is mounted at an angle, pointed down at the powder bed (see Figure 5). An optimal working angle is not established. Achieving a vertical overhead view is unreasonable. In both machines the laser hardware blocks this view path. However, it is still assumed that the closer the camera is to be being pointed directly down, over the powder bed, the better. This is because the further the camera tilts from a vertical view of the powder bed, the greater the change in perspective that must be corrected.

When viewed at an angle, points on the powder bed seem deceptively larger the closer they are to the camera due to the perspective. This distortion causes inaccuracies when measuring characteristics of the heated area beneath the laser beam. Software can correct this perception issue (see Figure 6) and restore a view that better represents the relative sizes of objects in the image, but there is still a resolution concern: Points on the powder bed closer to the camera are captured with more resolution since they are larger in frame. A greater resolution image improves measurements such as size analysis because there are more pixels to base the measurements off. It appears from looking at the output of a perspective correction test that the software might be reducing the resolution of closer objects to adjust perceived size. If this is

the case, resolution, and ultimately measurement accuracy, is lost when compared with an overhead frame-filled view of the subject. Therefore, the camera is angled as close as possible to an overhead view of the powder bed while maintaining a complete view of the zone. This positioning optimization is especially important when using the FLIR A325 because the resolution is already relatively low at 320x240.[5]

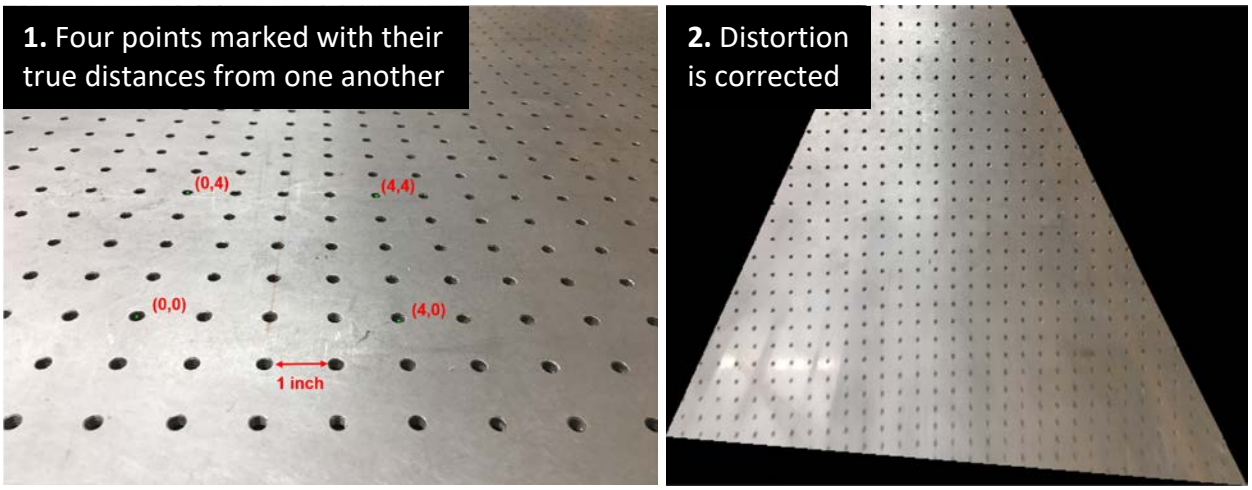

Figure 6: This demonstration shows how perspective distortion can be fixed with software calibration tools. The corrected image appears flat with the true relative size of objects restored.

Thermal imaging continues throughout the manufacturing process. Each captured image is sent to a program developed in LabVIEW for measurement extraction (see Figure 7). First, the images from the camera are calibrated to fix any lens or perspective distortion using the National Instruments Vision Development Module's calibration tools. The thermal grayscale images are then converted into binary data based on a threshold. Taking images from one camera, the program can isolate and measure up to three separate temperature regions simultaneously based on thresholds. The thresholds are set depending on what temperature zone the user is interested in measuring. Setting the threshold to pinpoint an accurate temperature region requires an understanding of the camera being used and the environment.

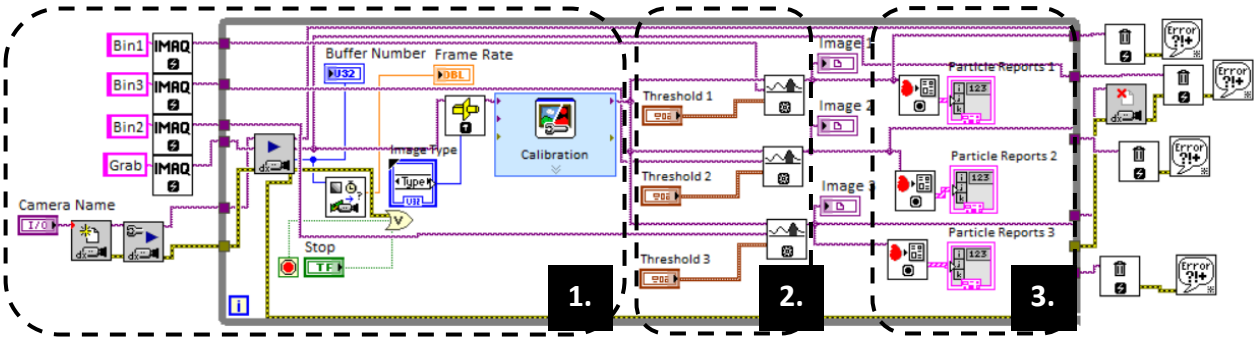

Figure 7: Displayed is a compressed overview of the LabVIEW image processing program.
1. Camera connection, image input, and calibration 2. Temperature thresholding
3. Temperature region measurement

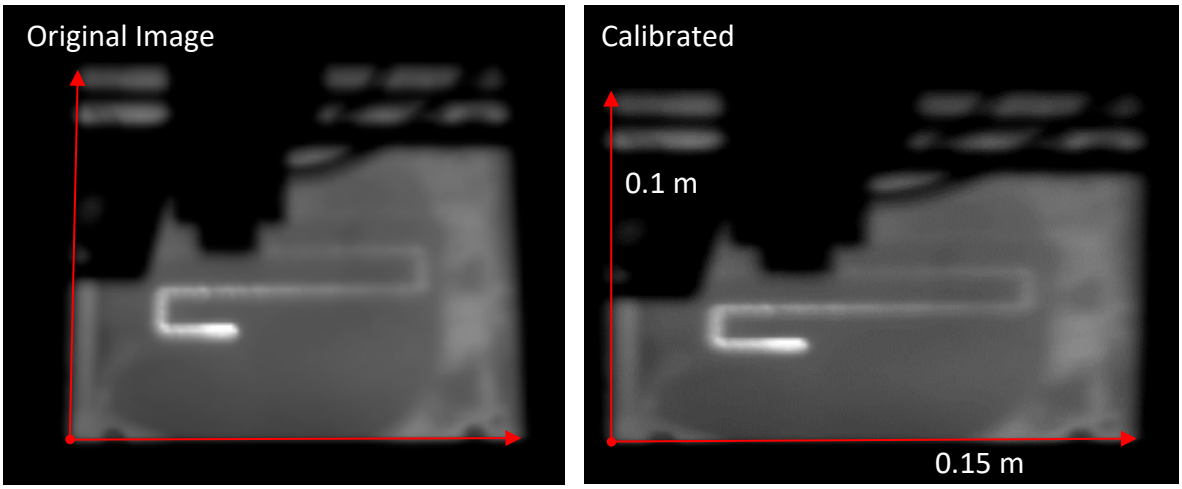

*Figure 8: (Pictured left) Thermal image taken from a test using the Plan-B machine with laser power set to 2.2 W and the scan speed running at 10 mm/s. The powdered material being sintered is a dark PA12 polymer. (Pictured right) Image after calibration to fix the view distortion. *It is important to note that this example is from recorded test footage. A version of the program seen in Figure 7 is modified to process .AVI video files instead of live camera feed. An overview of the modified program can be seen in Appendix A, Figure 22.*

Finding the temperature range displayed in the images is critical.[6] For FLIR cameras, like the A325, the software suite "FLIR Tools" can be used to obtain the image's temperature range. Once the range is known, the relationship between the software threshold and the temperature data from the thermal images can be determined. This can be achieved by taking a thermal image from a manufacturing test-run and isolating both the hottest and coldest points in the image with thresholds. The lower threshold from the isolated hottest point is the upper limit for thresholding the entire temperature range, while the upper threshold from the isolated coldest point is the lower limit for thresholding the entire temperature range. Specific thresholds in between the upper and lower limits of the image can then be obtained using interpolation assuming the image has a temperature linear color distribution.[7]

Camera resolution, and environmental emissivity are two important factors one should consider before thresholding. Both can impact the accuracy of temperature readings.[8][9]

Detector resolution determines the camera's ability to capture detail.[10] When observing sintering, loss of detail might lead to more error when measuring temperature regions. It is therefore a good idea to make sure the subject being captured fills as much of the camera frame as possible while remaining in focus. This takes full advantage of the camera's resolution.

Emissivity, or the ability of a surface to emit heat, impacts the perceived temperature of objects. The emissivity value for a specific material sits between 0.0 and 1.0 and is a ratio of how well the material radiates infrared energy, compared to a perfect radiator.[11] Thermal imaging accuracy is generally thrown off by low emissivity. If a material's emissivity is lower than 0.6, one

should not expect accurate results. However, most non-metals, like polymer-based powders used in SLS are decent emitters with emissivity values close to 1. Gathering accurate temperature readings from these materials is less problematic. [8] Small deviations can be accounted for in camera settings or FLIR Tools software. Beside the material properties, viewing angle can also affect emissivity. [11] For a flat subject, an angle of 45/50°, relative to a direct view, should not be exceeded in order to maintain measurement accuracy. [8] This provides another reason to make sure the camera is as close to a vertical orientation over the powder bed as possible.

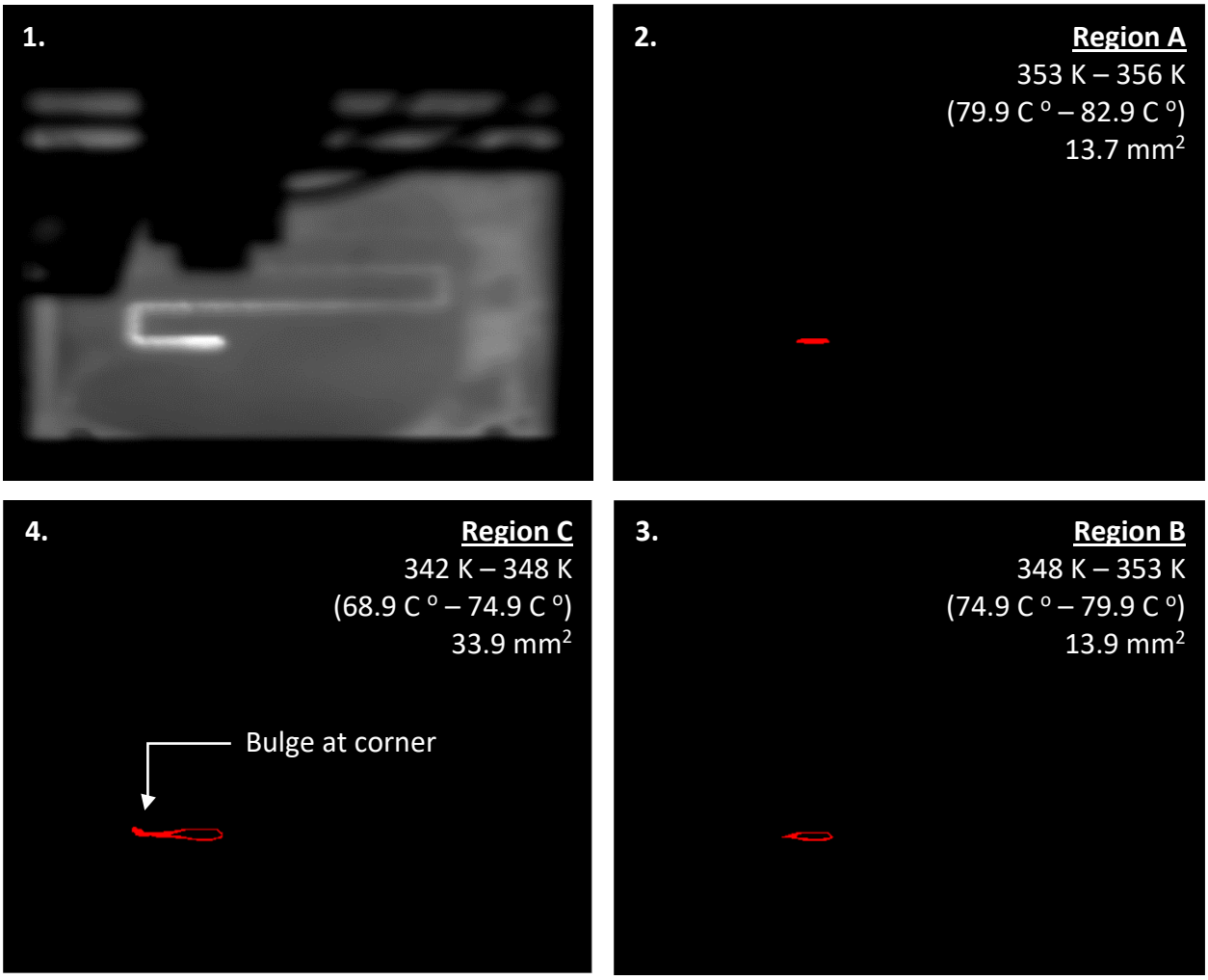

Figure 9: (Clockwise from upper-left) 1. The calibrated image from Figure 8 has a pictured temperature range of 306 K – 356 K (32.85 C °- 82.85 C °) with temperature linear color distribution. The dark PA12 powder used in this test is assumed to have an emissivity of 0.95 (like black plastic) [12] which is accounted for by adjusting the settings in FLIR Tools. 2. Directly under the beam of the laser is the hottest region. 3. Another temperature region is monitored between the hottest zone and the cooler outskirts. 4. A final threshold captures part of the warm trail left behind the laser's path. Notice the bulge on the corner that the laser passed. The ability to expose details like this, that might influence fabrication quality, shows additional use for the program.

Within Figure 9, one can see a demonstration of how images are taken and broken up into temperature regions by the program. After the regions have been establish by thresholds, each image is analyzed with particle analysis. This means measuring target areas based off the number of red pixels they consist of in the image. The number of red pixels is compared against the total number of pixels within a part of the image that has a known real-world area. Equation 1 delivers the real-world area of the temperature region based off the particle analysis report:

$$A_T = \frac{P_R}{P_{PB}} A_T \qquad \textit{Equation 1}$$

where P_R is the number of pixels that make up a specific temperature region part of the image, P_T is the total number of pixels in an area of the image where the real-world area is known (the powder bed area in this case), A_T is the known real-world area corresponding with the area selected for P_T, and $\mathrm{A_R}$ is the real-world area of the temperature region in question.

For the test shown in Figure 10, the total number of pixels is found for the powder bed area known to be 0.015 m^2. From the particle analysis and the known area, the following results can be obtained:

Region	P_R Region Pixels	P_T Powder Bed Pixels	A_T Powder Bed Real-World Area (m2)	A_R Region Area (m2)
A	248	271566	0.015	1.37E-05
B	251	271566	0.015	1.39E-05
C	613	271566	0.015	3.39E-05

Figure 10: Displayed is a table showing the pixel counts for each region from the tests in Figure 9 and the resulting real-world areas. The results are converted to mm^2 in Figure 9.

Raw particle analysis reports for each region can also deliver several other measurements. These can be seen in Figure 11.

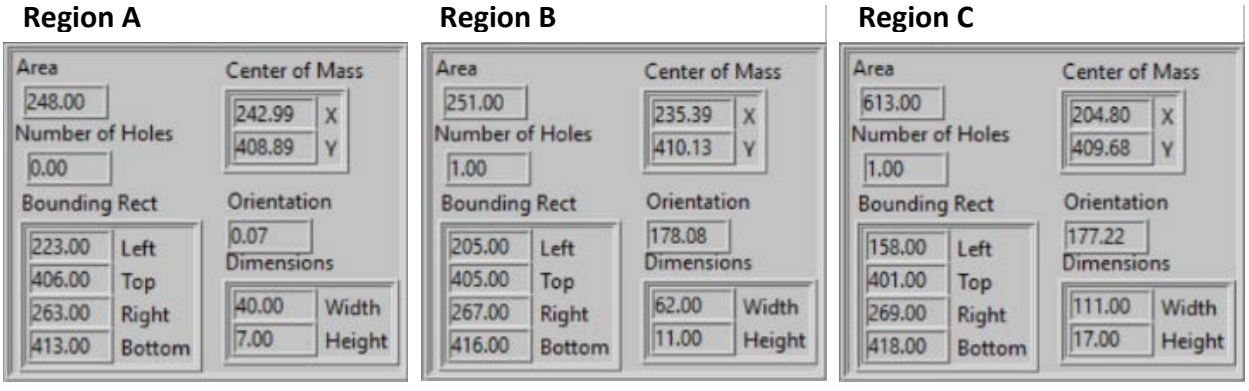

Figure 11: Each box shows the full particle analysis report for each region with a selection of different measurements. Notice that for region B and region C the number of holes is 1.00, while region A has no holes. This can be verified by looking at the image outputs in Figure 9. A view of the program's entire front panel can be seen in Appendix B, Figure 23.

6. Controller Component

The imaging setup, including the camera and vision program, is intended to be used as a sensor. Outputs from the particle analysis reports, seen in Figure 12, can be used to control the SLS manufacturing process. All the different outputs can be directly linked to a controller programmed within LabVIEW granting a significant amount of options and versatility. Figure 13 shows the results from particle analysis being sent to a controller SubVI.

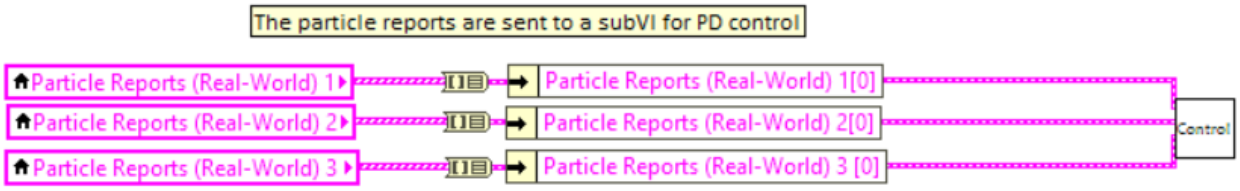

Figure 12: Three separate particle analysis reports for each region are sent into a controller SubVI.

Within the "Controller" SubVI block, one can pick measurements from each region's particle report to use in the control process. Figure 13 shows the area measurement being taken from a region's particle report for use in a PID (proportional-integral-derivative) control setup. Other measurements from the report, or combinations of measurements from different regions, might also serve as good inputs for control. For example, the "Center of Mass" measurement might be a promising input to use alongside a controller with area as an input. This is because certain scan patterns (like the corner in Figure 9) cause buildups of measured area behind the current position of sintering. These buildups, left behind the path of the laser, might sway a controller (with only area input) into incorrectly adjusting manufacturing at the laser's current position. By comparing the "Center of Mass" measurement from a hot region right below the laser (like Figure 9, Region A) to the "Center of Mass" from a cooler region (like Figure 9, Region C) one might be able to determine if a buildup has occurred. Some sort of response minimizing the buildup's impact on manufacturing control at the current sintering position might then be implemented. This is just speculation on how different inputs might be made useful. It also shows the control component's potential.

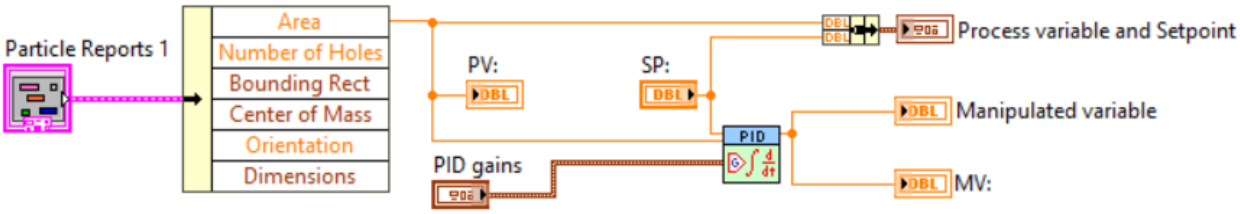

Figure 13: Outputs from all three particle analysis reports are available to use as sensor signals in the controller SubVI. An example PID controller is setup using area from one of the particle reports. "PV" is the process variable corresponding to the sensor signal, "SP" is the setpoint placed by the operator, "MV" is the manipulated variable, and "PID gains" hosts the tuning constants (proportional gain, integral time, and derivative time). The PID block holds the function.

For the PID controller example pictured in Figure 13, a desired area is denoted as the setpoint. Differences (the error) between the setpoint and the region areas measured during operation are then processed by each component of the PID function. The output manipulated variable adjusts the manufacturing process. Changes in temperature region area caused by adjustments are picked up by the sensor system and fed into the controller. This process runs with the goal of achieving a region area matching the setpoint.

Inside the PID function (see Equation 2), each of the three parts uses the error term $e(t)$, in a different way. The goal of the added responses is to create a manipulated variable signal, $u(t)$, that adjusts the manufacturing process so that, eventually, the area difference (error) goes to zero.

$$u(t) = K_p e(t) + K_i \int e(t)\,dt + K_d \frac{de}{dt} \qquad \textit{Equation 2}^{[13]}$$

The proportional component takes the area difference $e(t)$ and multiplies it by proportional gain term K_p to generate an output. Larger proportional gain is generally considered a way to achieve a faster response moving towards the setpoint. However, if the gain is too large it could lead to overshoots, or in drastic situations out of control oscillations. [14]

Unlike the proportional component, which only depends on the difference between the setpoint and measured area at one time, the integral component, $K_i \int e(t)\,dt$, sums up the area differences over time. [14] This means that if the difference in area between the setpoint and measured value is very small, the integral component will keep adding up this difference to develop an increasingly larger response over time. Assuming this response manipulates the sintering manufacturing process in the correct manner, the integral component will keep escalating to try to drive the area difference to zero as long as there is an area difference. For comparison, the proportional component might do barely anything in this situation because it will continuously generate an insignificant response based off the small amount of $e(t)$.

While the temperature region area is changing size, the derivative component, $K_p \frac{de}{dt}$, delivers a response dependent on the rate at which $e(t)$ changes.[14] For example, if measured temperature region area is rapidly approaching the desired setpoint area then the derivative component will register a rapidly decreasing $e(t)$ value which translates through the derivative as a negative value. This negative response will decrease the net response $u(t)$ to slow the rate at which the area is changing size so that there is not a drastic overshot of the setpoint.

The PID controller example shown in Figure 13 is not tuned and is currently just a placeholder. Since the example pictured in Figure 9 is from a recorded test, this controller has no production impact to study. To make this controller section functional the manipulated variable must be linked to an actuator during a live SLS manufacturing run.

7. Actuation Methodology Overview

Manipulating laser energy density is the actuation strategy investigated for both Plan-B and MACS Machine. By adjusting laser energy density, one can change the characteristics of temperature regions during manufacturing. Ultimately, this might grant the power to influence fabrication results because laser density is a key manufacturing parameter affecting the quality of particle sintering.[15] Equation 3 outlines how characteristics of the laser affect energy density, where E_L is the laser energy density, P_L is the laser power, A_L is the laser spot size, and S_L is the laser scan speed.

$$E_L = \frac{P_L}{A_L S_L} \qquad \textit{Equation 3}^{[15]}$$

Different variables in Equation 3 are picked for manipulation on each machine due to differences in ease of implementation. For the Plan-B machine, laser scan speed S_L is chosen for manipulation. Increasing laser scan speed S_L decreases the energy density E_L in an inverse proportional relationship. (An example showing the impact scan speed has on Plan-B's measured temperature can be seen in Figure 14 while a theoretical graph of Plan-B's energy density vs scan speed is provided in Figure 15). For the MACS Machine, laser power is the parameter targeted for adjustment. By increasing laser power P_L one theoretically proportionally increases the laser energy density E_L which can be seen in Figure 16.

Both actuation strategies are accomplished mostly through programming. The possibility of changing laser spot size is ignored onboard both the MACS Machine and Plan-B. Additional optical hardware might be required to control this variable for most machines.

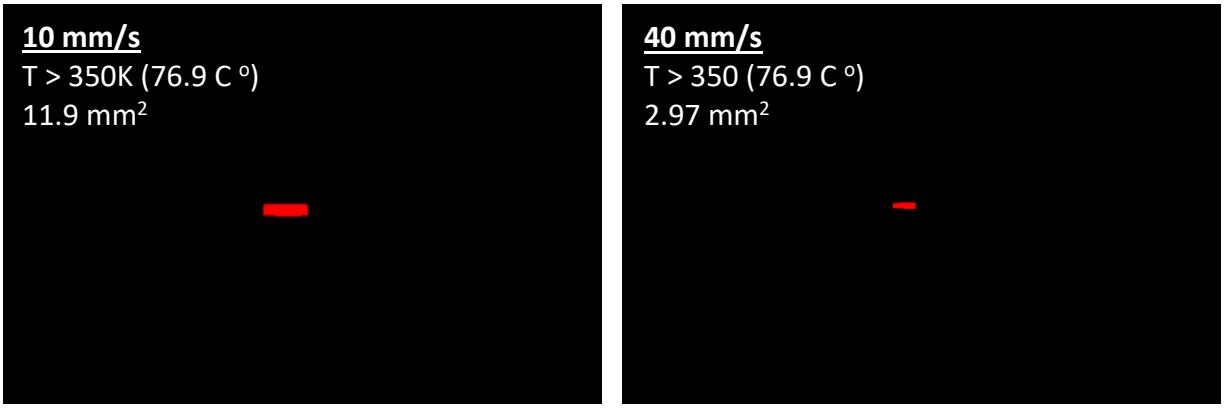

*Figure 14: This comparison shows how scan speed impacts measured temperature on the Plan-B machine. Seeing smaller temperature region size at a faster scan speed indicates how increasing scan speed leads to less energy density. This trend is visualized in Figure 15. *Note: a comparison between the 10 mm/s image here and the results shown in Figure 9 (same test conditions) shows how image resolution can impact the sensor system's measuring ability. These examples are from lower resolution samples. The area results have been impacted.*

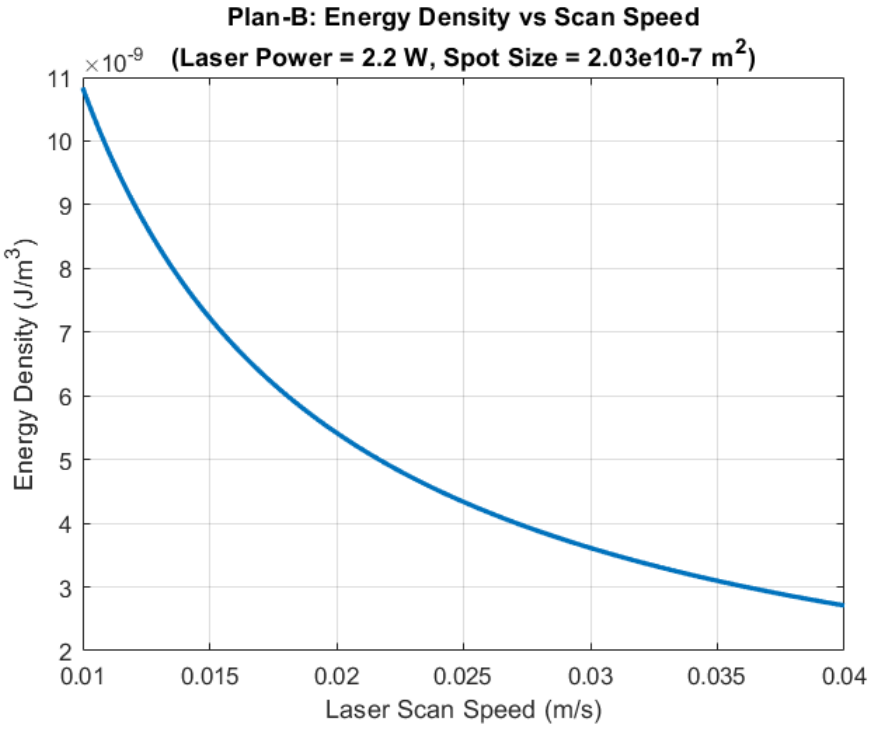

Figure 15: This graph, based off Equation 3, shows how increasing laser scan speed on the Plan-B machine leads to lower energy density.

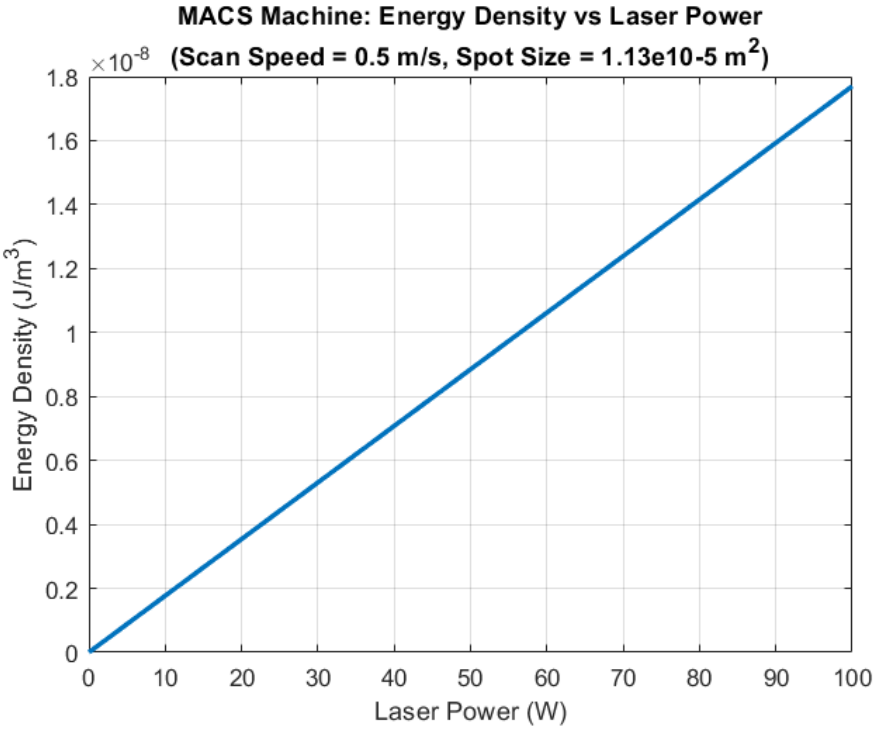

Figure 16: Increasing laser power on the MACS Machine proportionally increases energy density.

8. Plan-B Laser Scan Speed Actuation

To enable laser scan speed adjustments onboard Plan-B during the manufacturing process, a scheme is pursued to modify the system programing to allow speed changes potentially after every line of g-code. G-code stands for "geometric code" and instructs machines how to fabricate a specific product.[16] Within a line of g-code there are several variables used to guide the machine's behavior during production. For example, Plan-B uses the X and Y variables from each line of g-code to position the laser over the powder bed (like a coordinate plane).

The Plan-B machine operates using a Megatronics Atmega2560-16AU microcontroller board. This controller's programming is Arduino based (C/C++). It can be modified and deployed to Plan-B using the Arduino IDE.[17] During manufacturing, manipulated variable signals from the controller component in LabVIEW can be sent to the Megatronics board using I2C protocol. To enable I2C protocol, the board is physically connected to the computer hosting the LabVIEW sensor program using a Devantech USB to I2C interface module.

During printing, Plan-B executes the g-code inside a "while" loop, line by line. A variable already exists in Plan-B's system programming to set laser scan speed for a whole print. This variable's value can be changed inside the printing loop, opening the possibility to change the laser scan speed each time a new line of g-code is executed. However, the physical distances covered between each line of g-code are typically not constant. Depending on the object being fabricated, certain laser movements might be relatively long but defined by only a couple lines of g-code. This means that if laser scan speed is adjusted after the execution of every line of g-code, for sections where relatively long movements are only defined by a few lines, few adjustments can be made. To work around this, a program is developed to increase the number of g-code lines defining such sections. This way, if a relatively long scan path is defined by only a few lines of g-code, the path will be sliced into smaller distances (made up of more lines of code) creating more points for speed adjustment.

A MATLAB program (seen in Appendix C) is developed to take the entire g-code prepared for an object queued for fabrication and increase the number of code lines. The expanded g-code is then sent to Plan-B for printing. A desired minimum distance defined between g-code lines can be specified inside the expander program. An example of how the program works can be seen in Figure 17.

Further modification can be made to Plan-B's system programming to ensure that speed adjustments only happen after the specified distance has been traveled. This is done because certain geometric paths, like curves covering even just small distances, might still be defined by a lot of code lines (each line then moving the laser shorter distances then the distance specified within the expander program). By only permitting scan speed variations after a constant distance has passed, the entire control system might become more predictable and easier to tune.

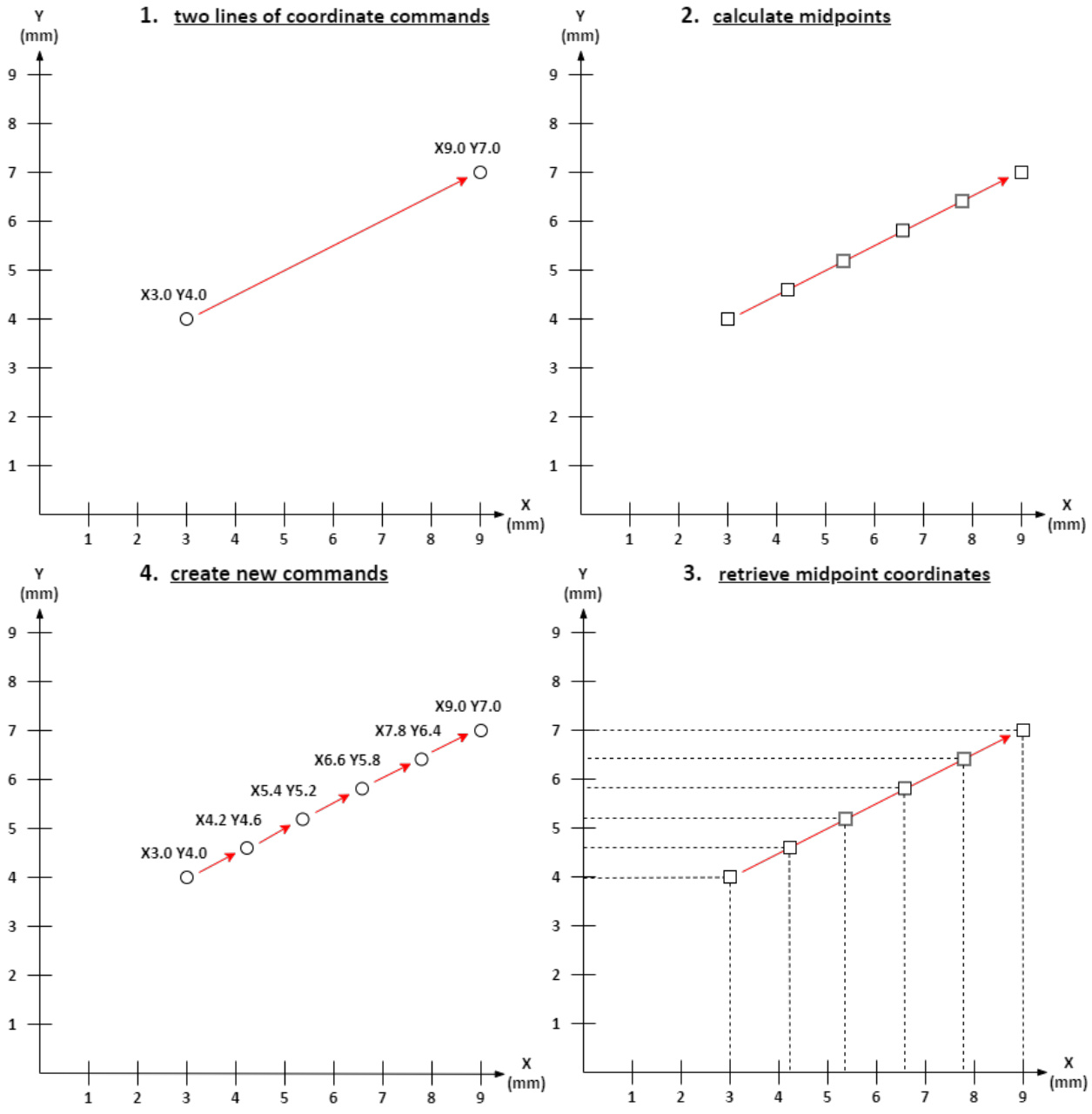

Figure 17: (Clockwise from upper-left) 1. Diagonal line made up of two commands is more than one millimeter in length. About one millimeter is the target distance sought between each command in this example. 2. The distance between the two points is calculated using Pythagorean theorem. This distance (if a non-integer) is rounded down to the nearest integer and a matching number of midpoints are created (including the start and end point.) 3. The X and Y coordinates of the midpoints are captured. 4. Four new commands are created and placed between the original two. An exact distance of one millimeter is not achieved between each command due to rounding, and the reality that unless the distance between the original diagonal commands is a perfect square, generating only one-millimeter spaced commands is not possible.

9. MACS Machine Laser Power Actuation

MACS Machine's software consists of a state machine (programmed in LabVIEW) responsible for coordinating system operations. Altering the state machine's working process might enable control over laser power during manufacturing.

The CO^2 laser on MACS Machine is controlled by a SCANLAB RTC®5 interface board. Laser commands carried about by the board are arranged using SCANLAB's custom LabVIEW blocks inside the state machine. Two types of commands are used on the interface board: list commands and control commands. List commands are stacked in a list (hence the name "list command") and placed in a buffer where they are carried out, one by one, after a list execution command is sent. Control commands are designed to execute immediately.[18]

The board can control the laser power (through pulse variation) with both list and control commands.[18] Adjusting laser power with a list command is an undesirable strategy because the instruction might be forced to wait for other list commands to process first. A list command must always, at least, wait for an execution command before running. This time delay might complicate tuning the control component. Therefore, using a control command to adjust laser power appears to be the better option because it is supposed to execute immediately. The manipulated variable from the control component will therefore almost instantly influence sintering. However, there are situations where control commands cannot execute. Certain types of list commands, called short list commands, obstruct the execution of control commands.[18] Although not all list commands cause obstruction, the possibility of interference means that it might be advantageous to find a point where the laser power adjustment can be processed alone.

Within the original state machine (see Figure 18), g-code, which instructs the machine in how to fabricate a specific product, is sorted by the "G" variable into either a marking command creation sequence or a jump command creation sequence. These sequences of list commands accumulate into one single list until executed. Once a g-code line with a jump is received that also contains an increase in the "Z" variable, the list is executed. This change in the "Z" variable corresponds to the end of an entire powder layer. If the laser power adjustment command is sent at the end of the execution of the list, it seems that there is no possibility it will be obstructed by a potential short list command. However, this strategy is not useful in the original state machine. List commands are accumulated to fabricate an entire layer, which means that laser power can only be adjusted once every new layer at unpredictable times.

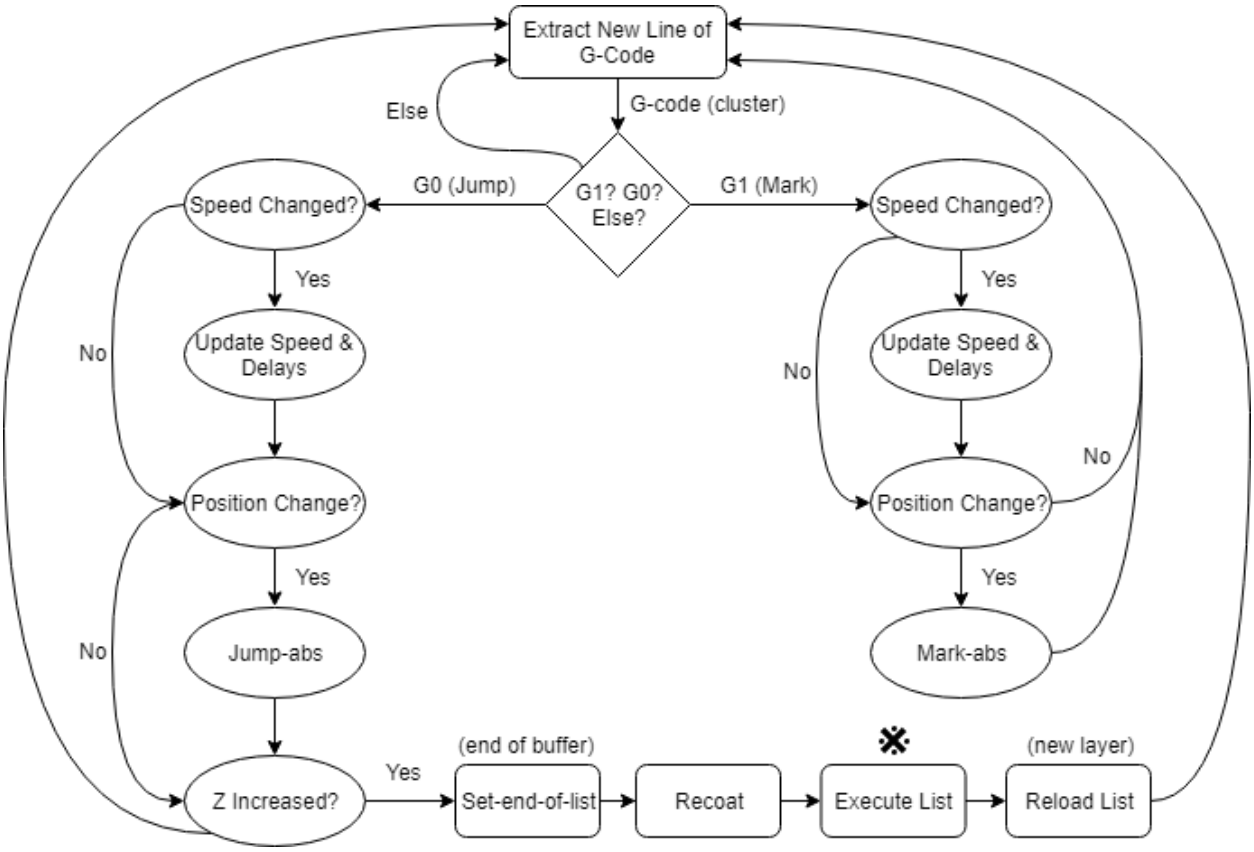

Figure 18: In the original state machine, the g-code only executes when a code line with a jump is received that also contains an increase in the "Z" variable.

By modifying the state machine to execute the list of g-code related commands more often, one could theoretically open more guaranteed opportunities to change laser power. Figure 19 shows an alteration plan for the state machine's g-code processing procedure that would permit assured laser power adjustments more often. These adjustments would happen after a set laser scan distance, specified by the machine operator, is covered.

To enable this capability, a program called "Measure" is added to determine the total laser scan distances specified by the g-code during the g-code processing procedure. Once the specified scan distance has been reached by list commands waiting to be executed, a laser power control command will be administered followed by the execute list command. In this way, a given laser power adjustment will be made from a manipulated variable determined by measuring the impacts of a previously executed list. The impact of a specific power adjustment will influence fabrication on the scan path of the command list executed after the laser power control command is administered. Adjustments occur after the same distance every time, except for situations when a layer ends and the remaining scan distance is less than the operator defined value. Assuming the laser scan speed is constant, the time between laser power adjustments also becomes constant. This will theoretically make the entire control system more predictable.

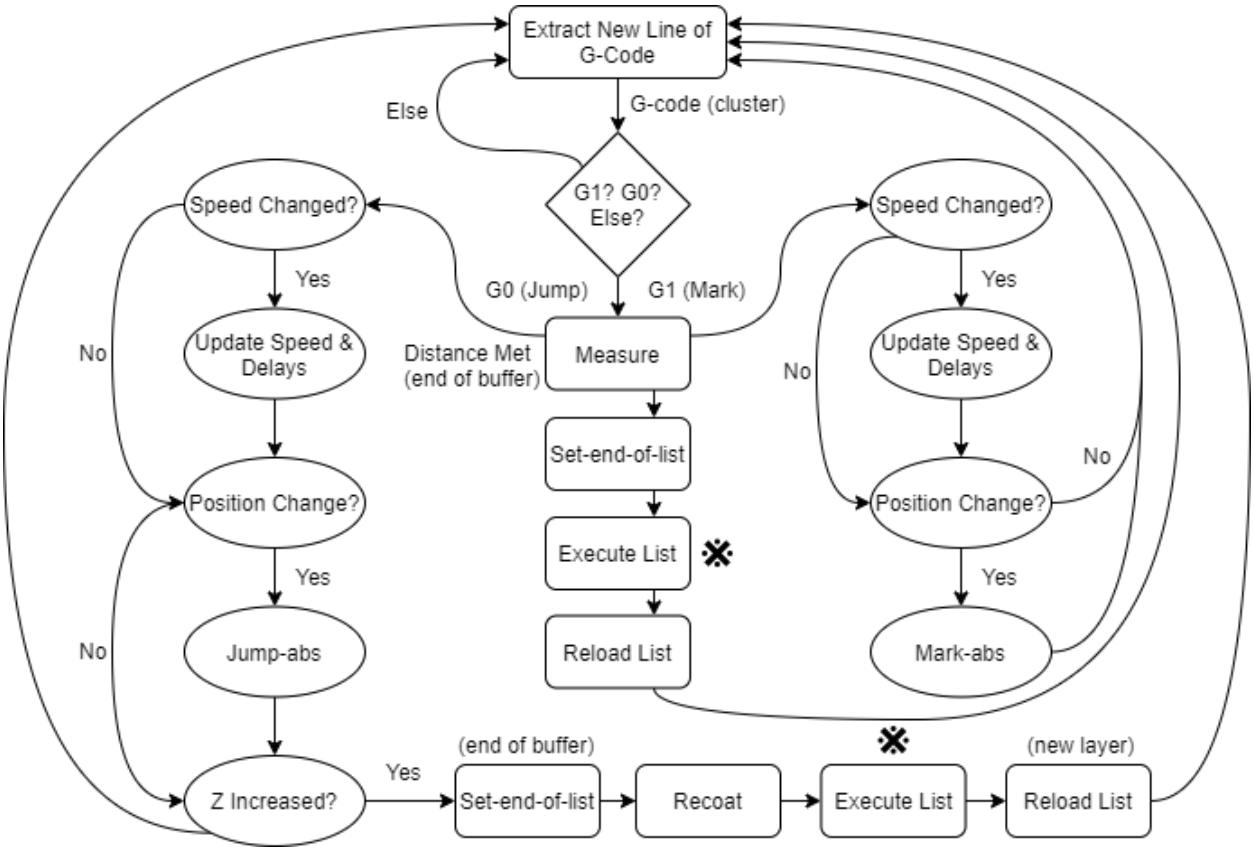

Figure 19: The modified software executes g-code after a user-defined distance is covered enabling laser power adjustments to be made more frequently. Adjustments occur right before the "Execute List" points, when a previous series of list commands have finished executing.

This actuation strategy can also make use of the g-code expander program (explained in Figure 17). For MACS Machine, situations might also exist where relatively long distances are defined by only a few lines of g-code. There could be scenarios where the state machine measurement step confirms that the cut-off distance specified by the user has been met but the scan distance, defined between the last and second to last lines of g-code, is still significantly longer than desired. Using the g-code expander program one can counter this by slicing up these longer scan paths into more lines of g-code.

Connecting this actuation assembly with the rest of the feedback control system should be relatively straightforward. This modified state machine maintains compatibility with the image processing program and control component since all these packages are LabVIEW-based.

10. Discussion

The control system variations designed for implementation on the MACS Machine and Plan-B are untested as fully connected items. However, one can find versatility and potential value in the designs when considering how certain components are intended for use on both machines, the software-modular nature of most of the programming, and the speculation of actuation strategies that require little-to-no additional hardware. Several system improvements are suggested based on the performance of components that received isolated testing.

Certain components were designed for use on both machines. The LabVIEW based sensor assembly can be configured to process live thermal camera feed, isolate separate temperature regions, and deliver measurement reports for any SLS machine where it can view the powder bed properly. The MATLAB based g-code expander program does not need significant modification to fit its role in the separate machine actuation strategies. These two items were intended to play some part in enabling feedback control onboard both SLS machines. This usefulness across the two different machines demonstrates design versatility.

Most software throughout the overall control system is designed to be modular and editable. LabVIEW's system-oriented programming environment and its variety of virtual instruments enable this quality to an extent. Different programs such as the image processor, the control component, and MACS Machine's state machine are all LabVIEW based and easily connected. The entire image processing program is completely contained and editable within LabVIEW. This eliminates complications that might arise from coordinating several different independent programs. Pieces like the image processing section, can be taken and integrated for use on other machines that use LabVIEW. This inter-compatibility and modularity also shows some versatility.

Other parts of the control system design are meant to deliver value as speculation. For example, although the actuation plans for each machine are not fully proven, they serve as potential strategies to influence sintering on SLS machines while requiring little extra hardware. The implementation of the actuation plan for Plan-B only requires a USB to I2C converter while the proposed actuation strategy for the MACS Machine only consists of software modifications. Both plans might prove useful as inspiration for low-cost approaches to actuation when designing control systems for relatable SLS/SLM machines.

Improvements can be made to make the control system potentially more flexible and effective. Using a thermal camera with higher image resolution, better temperature sensitivity, and faster framerate might significantly improve the entire systems capabilities. With a higher image resolution, temperature regions could consist of more pixels granting more accurate measurement results (see Figure 20). Better temperature sensitivity could enable the capability to isolate very specific temperature ranges if needed. Finally, with a higher camera framerate,

an increased rate of measurements could potentially be obtained and fed into the controller, which might then offer performance improvements. Given the many potential benefits, it seems like getting the best camera possible is an obvious move. However, high-end thermal cameras are currently prohibitively expensive so there is a trade-off to consider.

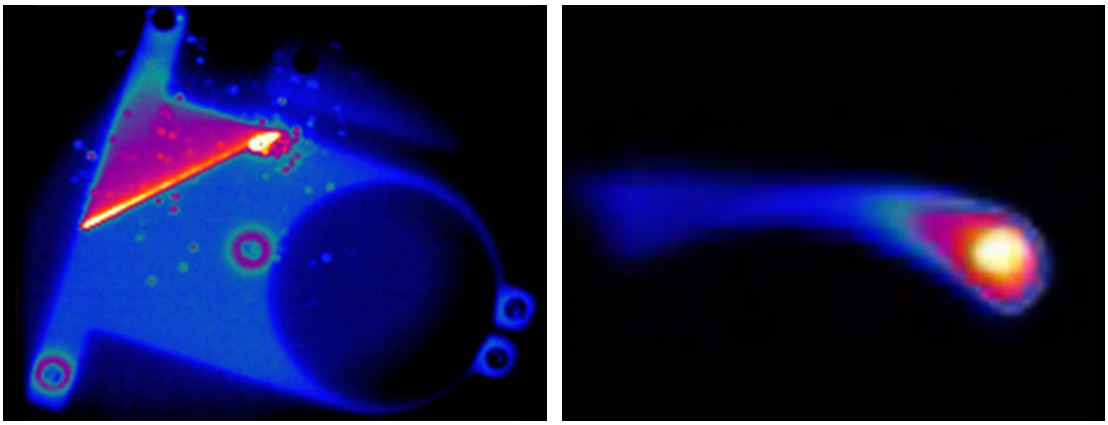

Figure 20: High end thermal cameras can provide more detail for accurate temperature region measurements. These images are taken from a high-speed thermal camera demo. [19]

Using a field programmable gate array (FPGA) to run the image processing and controller component programs might also deliver some performance benefits. FPGA offers the potential to speed up the response time of both the sensor and controller components with parallel processing. National Instruments produces an FPGA product that is specifically designed to deliver fast responses after analyzing camera feed (see Figure 21). However, there are three drawbacks to using National Instruments's FPGA cards: First, these cards are relatively expensive. Second, FPGA programming has a learning curve attached to it even with LabVIEW integration. Finally, not all SubVIs in LabVIEW can be deployed to the FPGA.

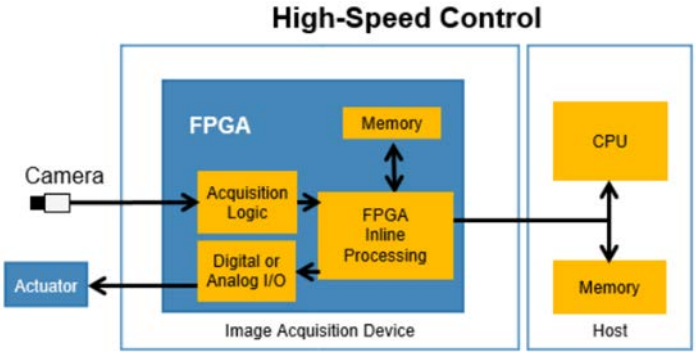

Figure 21: The diagram shows the processing sequence for the "PCIe-1473" card. This card takes Camera Link data and processes the images on an FPGA.[20] *This theoretically enables faster control responses.*

Conclusion

This report covered the design of a versatile feedback control system for potential use across different laser-based additive manufacturing machines with special focus placed on the functions of the individual components. Some of these components were shown to be capable of implementation across different SLS machines based on their compatibility with both Plan-B and MACS Machine. Adjustment possibilities across the designs were described with suggestions on how they might contribute to a thorough investigation of the potential benefits feedback control can offer SLS.

Several key features within the sensor component were reviewed. Camera position flexibility, granted by use of software distortion correction and emissivity guidelines for thermal imaging, was explained to permit the implementation of the sensor component on any machine that offers a view of the powder bed no greater than $45/50^{o}$ from a vertical view. It was explained how the image processing program can isolate up to three regions defined by temperature after receiving image data. A demonstration was provided showing how properties, such as the size of certain temperature regions, can be determined. These measurements, across all three temperature regions, were then shown to be useful as potential process variables in a controller component.

Actuation strategies that target laser behavior to influence laser energy density during sintering were explained. For each SLS testbed, a separate method of influencing laser energy density during manufacturing was investigated. For Plan-B, a strategy to control the laser scan speed was covered. On MACS Machine, it was shown how a modification might permit laser power adjustments. Both actuation plans were shown to work by taking advantage of the way the testbeds process g-code. A program designed to take g-code files and enforce a maximum allowable travel distance between each set of code lines was presented as a method of improving performance for each laser actuation plan. These strategies were shown to require minimal machine hardware additions.

References

[1] S. Fulga, A. Davidescu, and I. Effenberger, “Identification of in-line defects and failures during Additive Manufacturing Powder Bed Fusion processes,” *MATEC Web of Conferences*, vol. 94, p. 03005, 2017.

[2] K. Florio and K. Wegener, “A Review on Monitoring and Feedback Control for Ceramic SLM Processes Studies on Mechatronics Institute of Machine Tools and Manufacturing Swiss Federal Institute of Technology (ETH) Zürich Supervision A Review on Monitoring and Feedback Control for Ceramic SLM Processes List of Contents,” 2018.

[3] D. Hu and R. Kovacevic, “Sensing, modeling and control for laser-based additive manufacturing,” *International Journal of Machine Tools and Manufacture*, vol. 43, no. 1, pp. 51–60, Jan. 2003.

[4] P. Mercelis, Jean-Pierre Kruth, and Jonas Van Vaerenbergh, “Feedback control of selective laser melting,” *Semantic Scholar*, 2016. [Online]. Available: https://www.semanticscholar.org/paper/Feedback-control-of-selective-laser-melting-Mercelis-Kruth/4d65e479bf7a0b1637405bc773dee47fe996a8f6. [Accessed: 20-May-2020].

[5] FLIR, “FLIR A325sc Thermal Camera for Real-Time Analysis | FLIR Systems,” *www.flir.com*. [Online]. Available: https://www.flir.com/products/a325sc/. [Accessed: 20-May-2020].

[6] Fluke Corporation, “10 Things You Need To Know About Thermal Imagers | Fluke,” *www.fluke.com*. [Online]. Available: https://www.fluke.com/en-us/learn/blog/thermal-imaging/10-things-you-need-to-know-about-thermal-imagers. [Accessed: 20-May-2020].

[7] FLIR, “What happens when I select histogram equalization as the image presentation in FLIR Tools?,” *www.flir.com*. [Online]. Available: https://www.flir.com/support-center/Instruments/what-happens-when-i-select-histogram-equalization-as-the-image-presentation-in-flir-tools/. [Accessed: 20-May-2020].

[8] INFRARED TRAINING CENTER, “Introduction to Thermography Basics,” Infrared Training Center, Aug. 2014.

[9] Sofradir-EC Inc., “White Paper: Understanding Infrared Camera Thermal Image Quality,” *www.electricnet.com*. [Online]. Available: https://www.electricnet.com/doc/understanding-infrared-camera-thermal-image-0002. [Accessed: 21-May-2020].

[10] POWER, “How important is IR detector resolution?,” *POWER Magazine*, 15-Apr-2006. [Online]. Available: https://www.powermag.com/how-important-is-ir-detector-resolution/. [Accessed: 21-May-2020].

[11] Fluke Corporation, “How Emissivity Affects Thermal Images,” *www.fluke.com*. [Online]. Available: https://www.fluke.com/en-us/learn/best-practices/measurement-basics/thermography/how-emissivity-affects-thermal-images. [Accessed: 21-May-2020].

[12] ThermoWorks, “Infrared Emissivity Table | ThermoWorks,” *Thermoworks.com*, 2016. [Online]. Available: https://www.thermoworks.com/emissivity-table. [Accessed: 21-May-2020].

[13] K. Johanåström and R. Murray, *Feedback Systems*. 2019.

[14] National Instruments, “PID Theory Explained - National Instruments,” *www.ni.com*. [Online]. Available: https://www.ni.com/en-us/innovations/white-papers/06/pid-theory-explained.html#section-38687283. [Accessed: 21-May-2020].

[15] R. K. Ganeriwala, “Multiphysics modeling of selective laser sintering/melting,” 2015.

[16] Autodesk, “Getting Started with G-Code,” *Autodesk.com*, 2019. [Online]. Available: https://www.autodesk.com/industry/manufacturing/resources/manufacturing-engineer/g-code. [Accessed: 21-May-2020].

[17] B. Meijer and R. Com, “MEGATRONICS v3.1 DATASHEET,” 2018.

[18] SCANLAB, “Installation and Operation The RTC ® 5 PC Interface Board, RTC ® 5-Express Board, RTC ® 5 PC/104-Plus Board and RTC ® 5 PCIe/104 board for Real Time Control of Scan Heads and Lasers,” Sep. 2014.

[19] Telops, “High-Speed Infrared Imaging of Metal Parts Fabrication by Additive Manufacturing,” *Telops*, 2017. [Online]. Available: https://telops.com/markets-applications/additive-manufacturing. [Accessed: 21-May-2020].

[20] National Instruments, “PCIe-1473 - National Instruments,” *www.ni.com*. [Online]. Available: https://www.ni.com/en-us/support/model.pcie-1473.html. [Accessed: 21-May-2020].

Appendix A

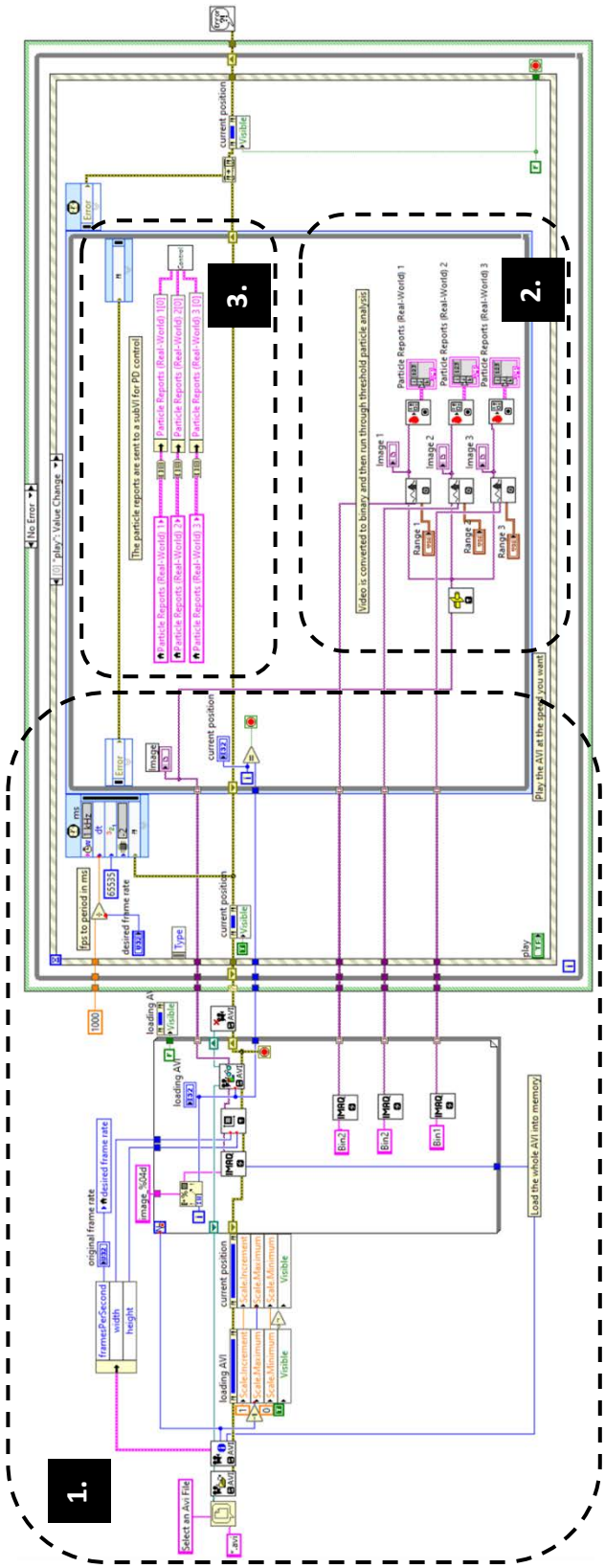

Figure 22: Displayed is an overview of the LabVIEW image processing program that uses AVI video input.
1. Load AVI video file and frame rate control
2. Temperature thresholding and measurement report
3. Sending report information to the controller SubVI (controller has no effect since input is just a video)

Appendix B

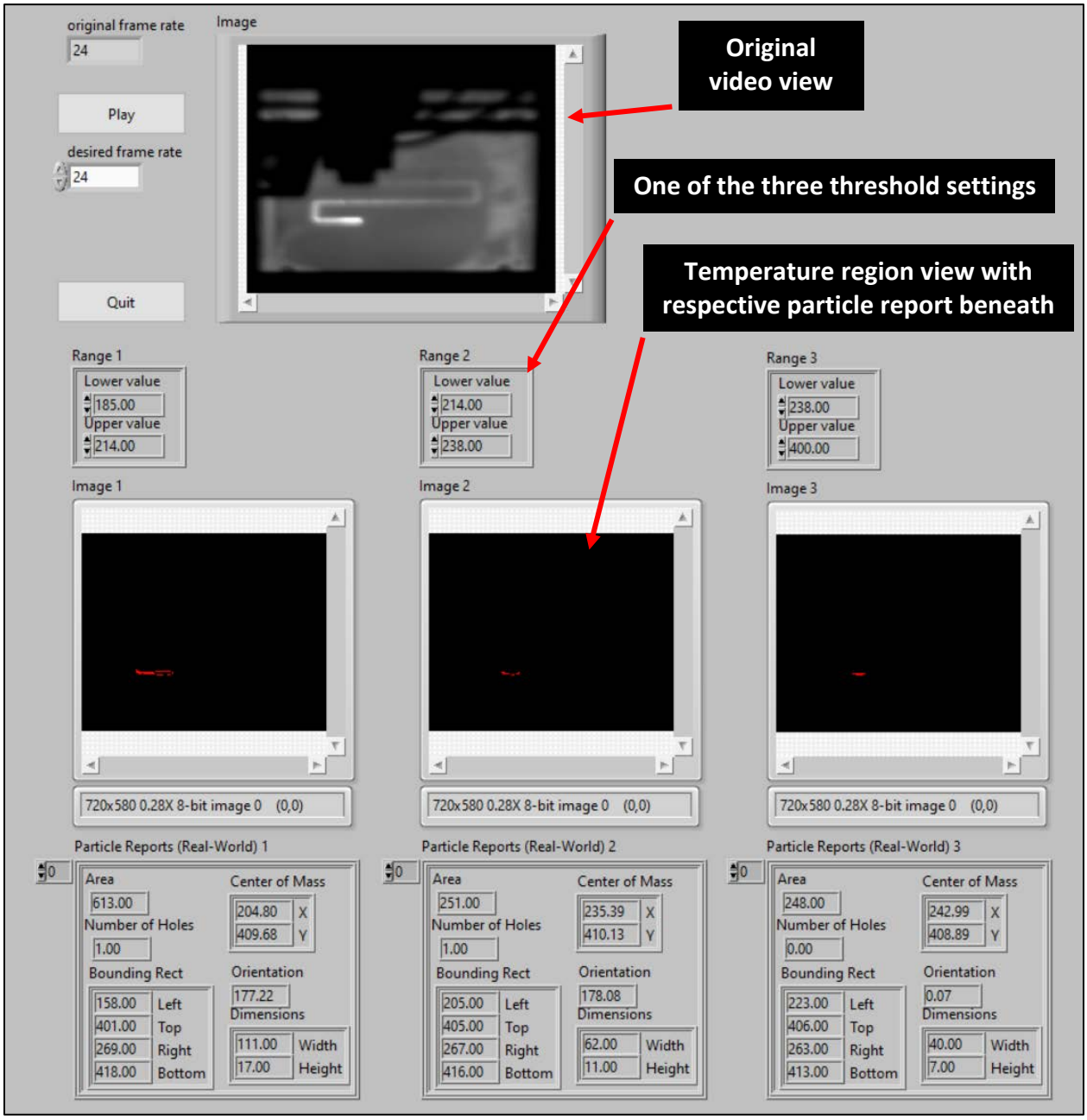

Figure 23: View of the AVI image processing program's front panel while running (Program displayed in Appendix A, Figure 22). Original AVI video view is at top while the three threshold region views are at bottom. Particle reports for each region are below their respective image views. Thresholds can be adjusted from this panel. The original version of this program that receives camera input instead of AVI video files is intended for use in the control feedback system. Its front panel is slightly different and can be seen in Appendix B, Figure 24.

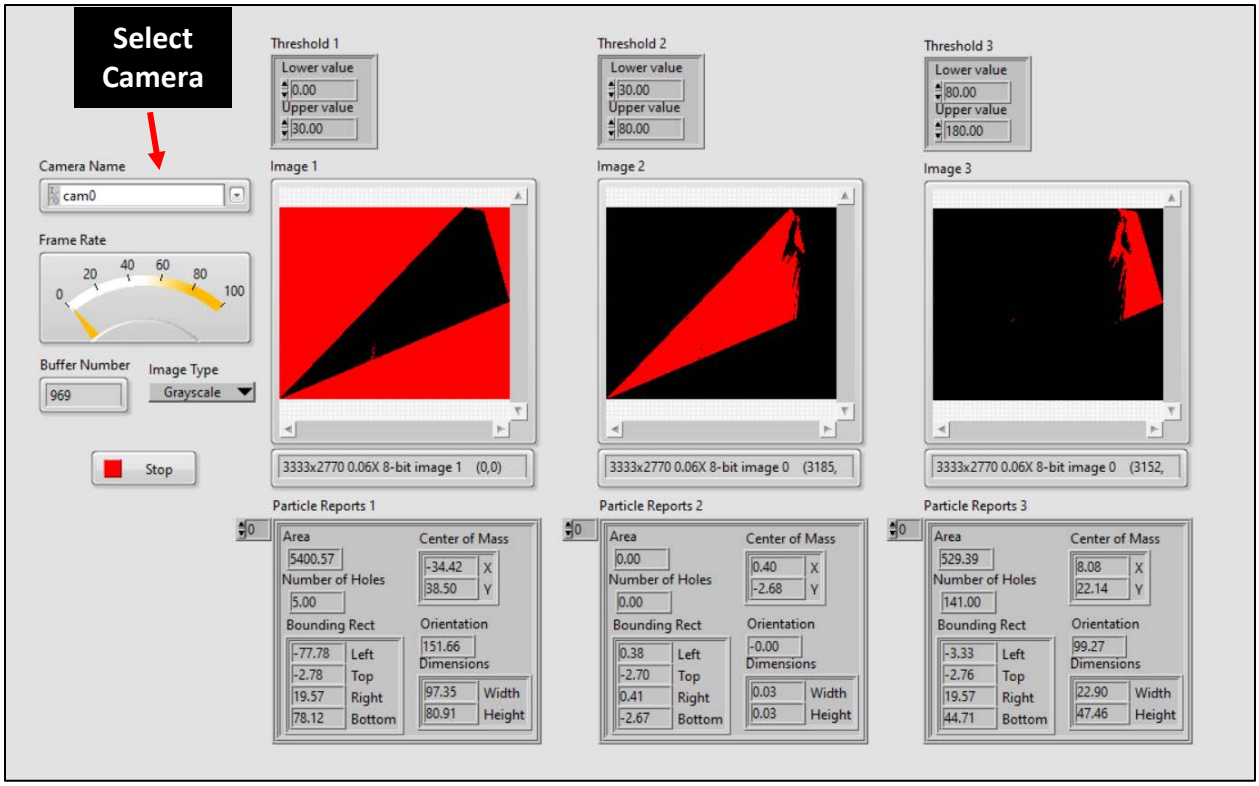

Figure 24: View of the camera input image processing program's front panel (program displayed in Figure 7). This panel consists of all the same features seen in Appendix B, Figure 23 except for the camera input option. While running, the camera framerate is displayed. The rectangular (almost triangular) shape seen in each of the region views is a heavily exaggerated use of the image calibrator to check for functionality.

Appendix C

```
clear
clc

%%%%%%%%%%%%%%%%%%%%%%%%%%%%
%'G-code Reader' takes code and sorts it into a column each by G-code variable
%ie: "Xcolumn, Ycolumn..." for further manipulation in MATLAB
%%%%%%%%%%%%%%%%%%%%%%%%%%%%

gread = fopen('inprint.txt','r');
gcode = textscan(gread,'%s','delimiter','\n');
fclose(gread);
lines = sum(cellfun('size',gcode,1));
gcode = gcode{1};
gcode = regexp(gcode,' ', 'split');
flatgcode = [gcode{:}];
[~,flatsize] = size(flatgcode);
Lines_limit = 10000;

Gcompare = "G";
Fcompare = "F";
Xcompare = "X";
Ycompare = "Y";
Ecompare = "E";

Gcolumn = zeros(Lines_limit,1);
Fcolumn = zeros(Lines_limit,1);
Xcolumn = zeros(Lines_limit,1);
Ycolumn = zeros(Lines_limit,1);
Ecolumn = zeros(Lines_limit,1);

Gcount = 1;
Fcount = 1;
Xcount = 1;
Ycount = 1;
Ecount = 1;

count = 1;

while count <= flatsize

  if strncmpi(flatgcode{1,count},Gcompare,1) == 1

      Gcolumn(Gcount,1) = str2double(strip(flatgcode{1,count},'left','G'));
      Gcount = Gcount + 1;

  elseif strncmpi(flatgcode{1,count},Fcompare,1) == 1

      Fcolumn(Fcount,1) = str2double(strip(flatgcode{1,count},'left','F'));
      Fcount = Fcount + 1;

  elseif strncmpi(flatgcode{1,count},Xcompare,1) == 1

      Xcolumn(Xcount,1) = str2double(strip(flatgcode{1,count},'left','X'));
      Xcount = Xcount + 1;

  elseif strncmpi(flatgcode{1,count},Ycompare,1) == 1

      Ycolumn(Ycount,1) = str2double(strip(flatgcode{1,count},'left','Y'));
      Ycount = Ycount + 1;
```

```
  elseif strncmpi(flatgcode{1,count},Ecompare,1) == 1

      Ecolumn(Ecount,1) = str2double(strip(flatgcode{1,count},'left','E'));
      Ecount = Ecount + 1;

  end

    count = count + 1;

end

Gcolumn(Gcount:end, :) = [];
Fcolumn(Fcount:end, :) = [];
Xcolumn(Xcount:end, :) = [];
Ycolumn(Ycount:end, :) = [];
Ecolumn(Ecount:end, :) = [];

%%%%%%%%%%%%%%%%%%%%%%%%%%%%
%'G-code Expander' takes X and Y information and cuts it up into smaller
%commands increasing the total number of G-code lines without changing the
%actual print
%
%Thank you to Jack Davis for the help in this section
%%%%%%%%%%%%%%%%%%%%%%%%%%%%

Xc = zeros(Lines_limit,1);
Yc = zeros(Lines_limit,1);
Xwrite = 1;
Ywrite = 1;
precision = 1;

for i = 1:(size(Xcolumn)-1)
    Xrange = Xcolumn(i+1) - Xcolumn(i);
    Yrange = Ycolumn(i+1) - Ycolumn(i);
    midpoints = sqrt(Xrange^2 + Yrange^2)/precision;

    Xinterp = linspace(Xcolumn(i), Xcolumn(i+1), midpoints);
    Yinterp = linspace(Ycolumn(i), Ycolumn(i+1), midpoints);

    Xinterp = round(Xinterp, 1);
    Yinterp = round(Yinterp, 1);

    Xc(Xwrite:Xwrite + size(Xinterp,2)-1,1) = Xinterp(1,:).';
    Yc(Ywrite:Ywrite + size(Yinterp,2)-1,1) = Yinterp(1,:).';
    Xwrite = Xwrite + size(Xinterp,2);
    Ywrite = Ywrite + size(Yinterp,2);
end

Ec = 1:size(Xc);
GMatrix = [Xc, Yc, Ec.'];
gwrite = fopen('outprint.txt','w+t');
formatSpec = 'G1 X%.1f Y%.1f E%.1f\n';
fprintf(gwrite,formatSpec,GMatrix.');
fclose(gwrite);
```